

ISCI, Volume 19

Supplemental Information

**Controllable Liquid-Liquid Printing
with Defect-free, Corrosion-
Resistance, Unrestricted Wetting Condition**

Lingli Min, Haohui Zhang, Hong Pan, Feng Wu, Yuhang Hu, Zhizhi Sheng, Miao Wang, Mengchuang Zhang, Shuli Wang, Xinyu Chen, and Xu Hou

Supplemental data

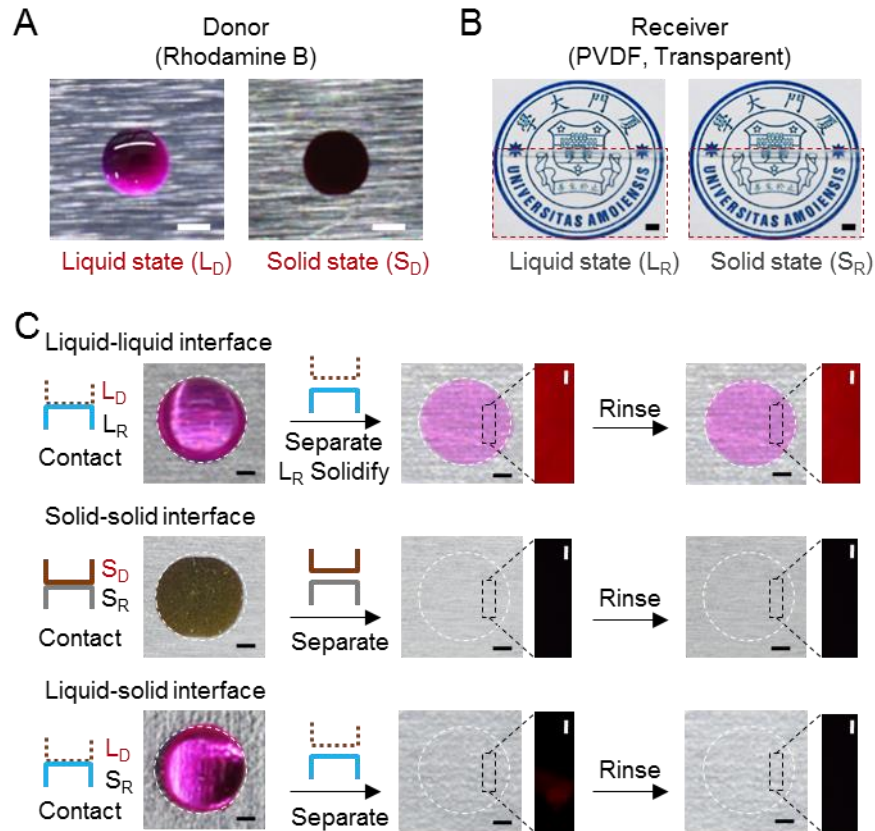


Figure S1. Substance transfer behaviors at different interfaces. (A) Photos of a donor liquid, Rhodamine B (RB) aqueous solution. L_D/S_D indicates the liquid/solid state of the donor. Scale bars: 0.5 mm. (B) Photos of a transparent PVDF receiver. L_R/S_R indicates the liquid/solid state of the receiver. The liquid state of the receiver is PVDF (acetone-DMAC). Scale bars: 0.5 mm. (C) Comparison of the stabilities among different printing approaches for substance transfer at liquid-liquid, solid-solid, and solid-liquid interfaces. The right insets (fluorescence images) show that only liquid-liquid interface delivered RB into PVDF receiver in the non-wetting system. Scale bars: 0.2 mm. Right insets scale bars: 50 μm . Related to Figure 1.

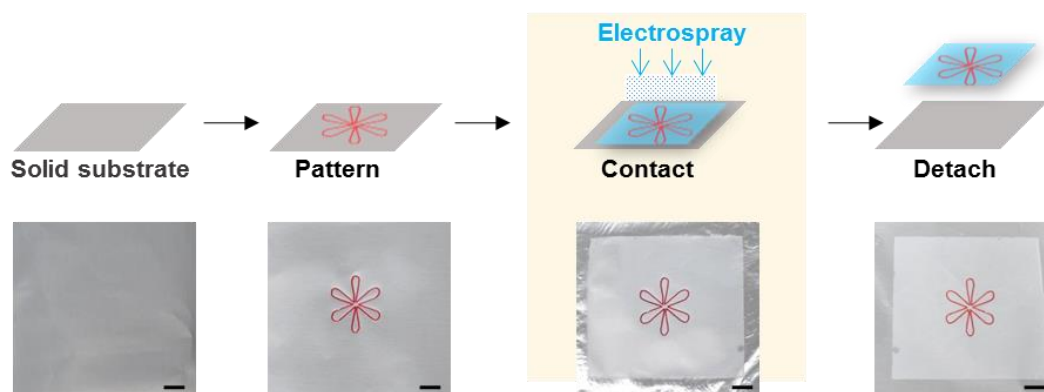


Figure S2. A typical liquid-liquid printing process *via* the electro spray. A pattern with donor liquid was written on a substrate (aluminum foil). During the electro spray process, the cross was transferred and delivered into the liquid receiver. The printed product could be easily peeled off from the donor substrate before or after the full solidification of the receiver. Scale bars: 5 mm. Related to Figure 1.

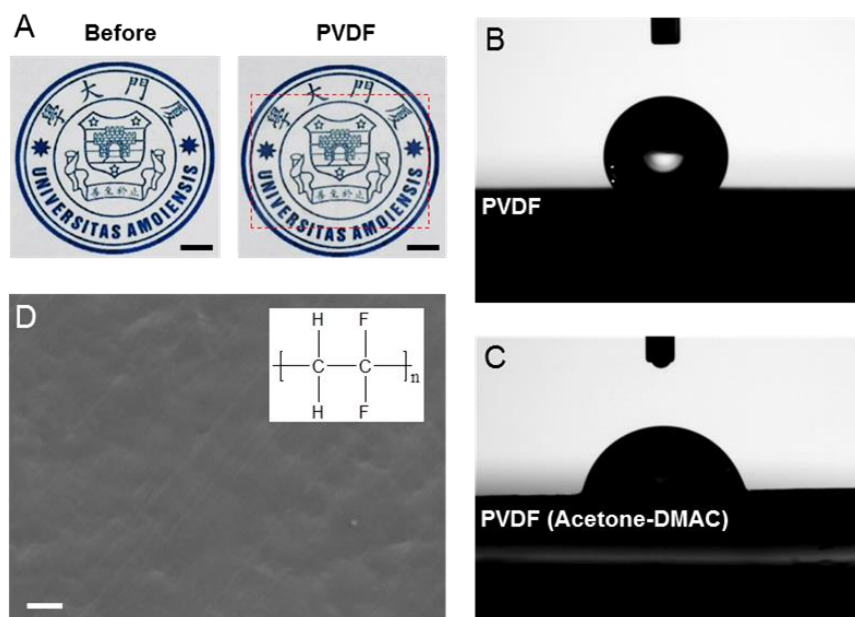


Figure S3. Characterization of the PVDF receiver. (A) Optical photos indicate the high transparency of the PVDF receiver (solid state, thickness, 3 μm). Scale bars, 5 mm. (B) The water contact angle of the solid state of PVDF. (C) The water receding angle of the liquid state of PVDF (acetone-DMAC). (D) The SEM image of the solid state of PVDF. Scale bar: 50 μm . Related to Figure 1.

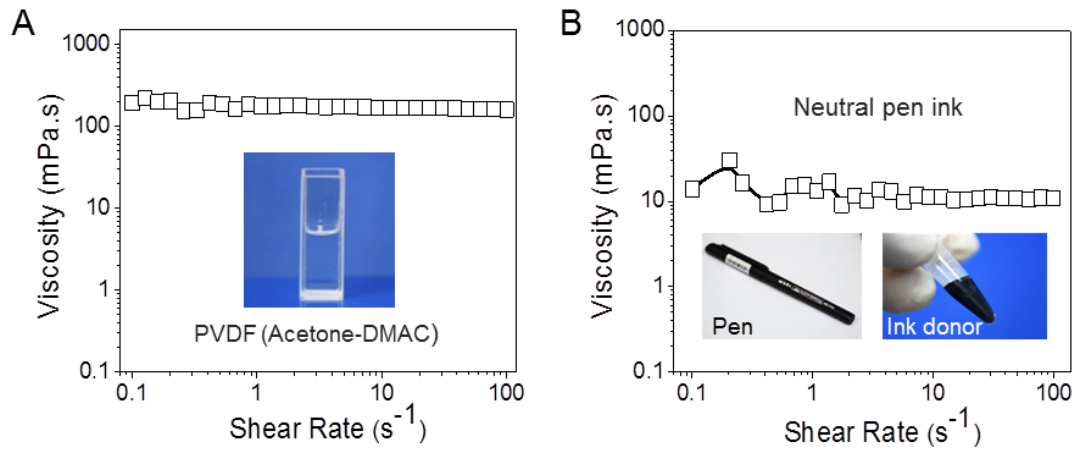


Figure S4. Rheological behavior of the receiver PVDF (acetone-DMAC) (A) and the neutral pen ink (B) used for Figure 3. Related to Figure 3.

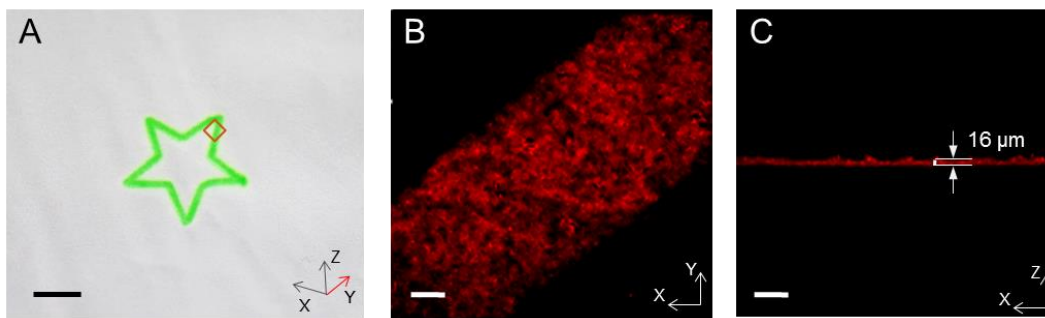


Figure S5. Characterization of the printed materials with star pattern in Figure 4B. (A) The liquid-liquid printing star after surface rinsing. (B, C) Laser confocal microscopy shows the 3D distribution of the donor solute in the receiver. The thickness of the receiver is 16 μm. Scale bars: 5 mm (A) and 100 μm (B and C). Related to Figure 4.

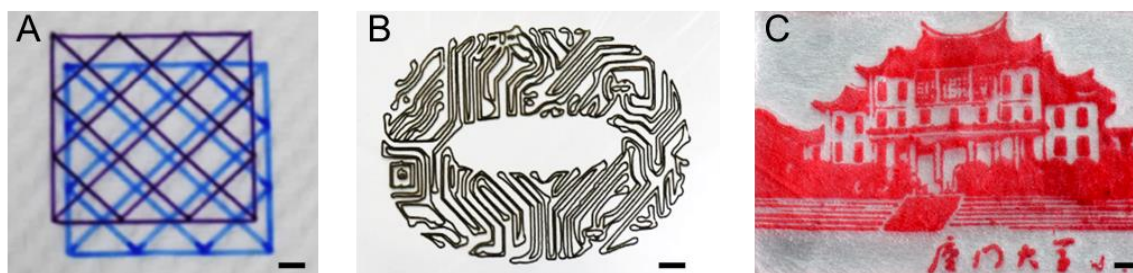


Figure S6. Examples of the liquid-liquid printing complex patterns. Crosslines (A), circular circuit pattern (B), the south auditorium building of Xiamen University (C). Scale bars: 5 mm. Related to Figure 4.

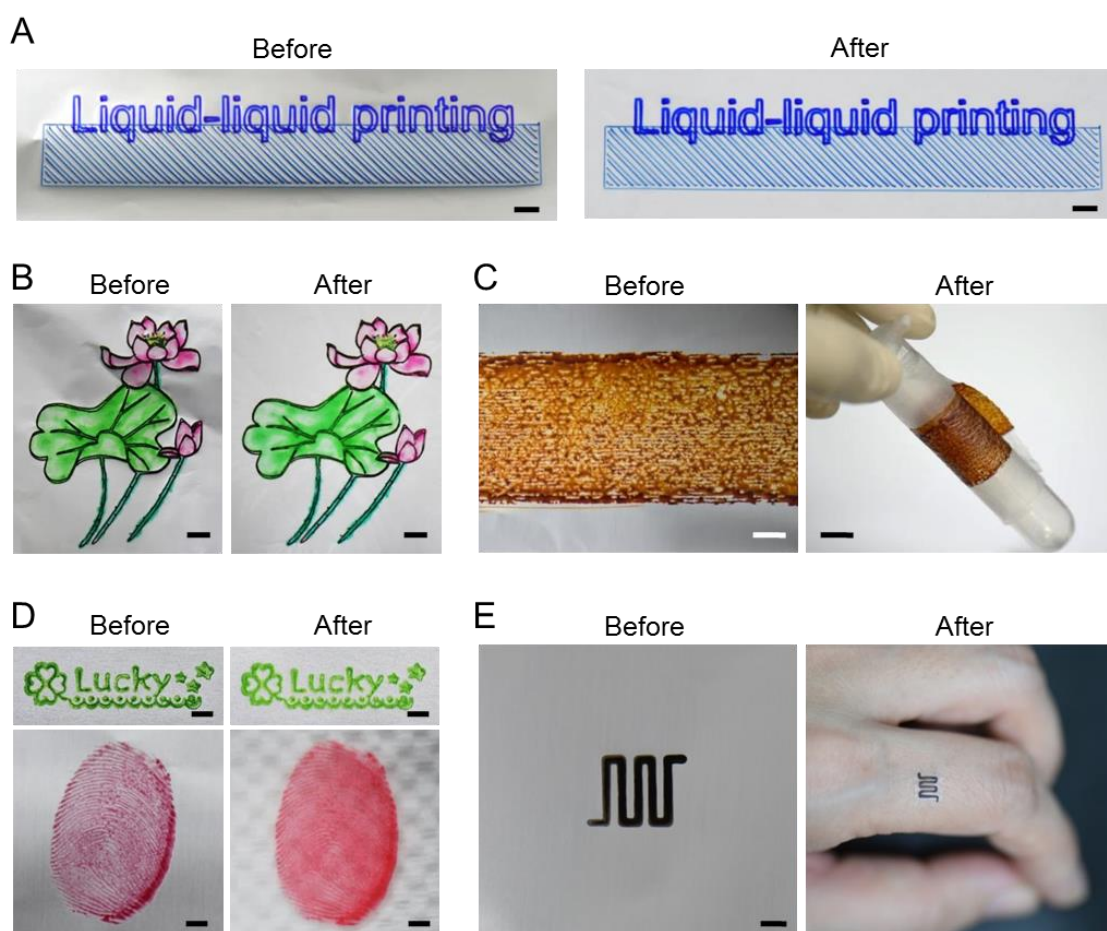


Figure S7. Various donor patterns before and after the liquid-liquid printing. A neutral gel pen donor (A), a color ink donor (B), an aqueous ferrofluid donor (C), a seal oil donor (D), and a lab-made composite donor (E). The printed products with the aqueous ferrofluid (C) and the lab-made composite donor (E) were attached to a centrifuge tube and a finger, respectively. Scale bars: 5 mm (A-C), 2 mm (D and E). Related to Figure 4.

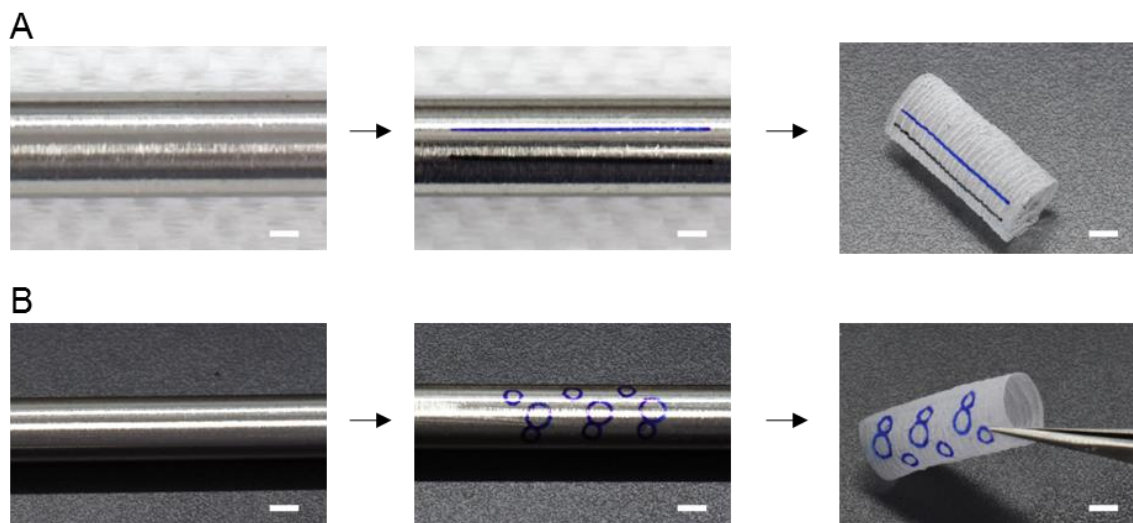


Figure S8. Typical processes of the liquid-liquid printing 3D structures. The Liquid-liquid printing achieves synchronization of 3D material preparation and inner patterning of lines (A) and circles (B). Scale bars: 3 mm. Related to Figure 4.

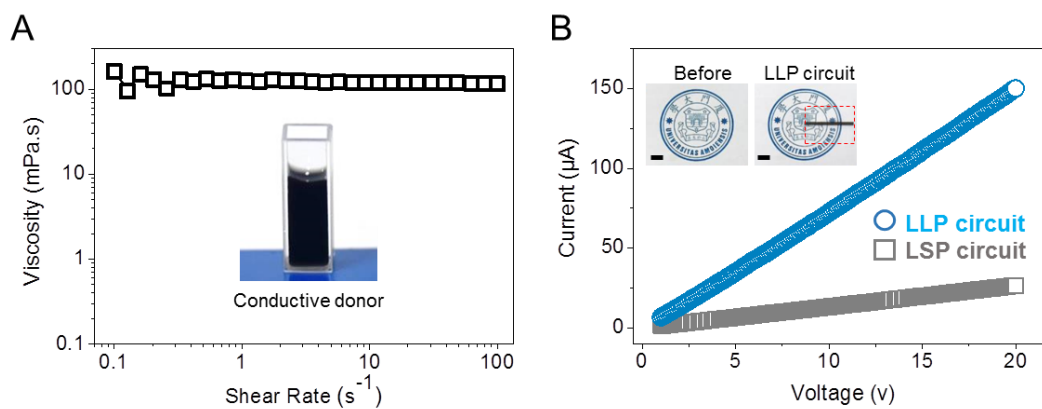


Figure S9. (A) Rheological behavior of the conductive donor. (B) The voltage-current tests of the printed circuits. Insets show the macroscopic optical images of the liquid-liquid printing flexible circuits. Scale bars, 5 mm. Related to Figure 4.

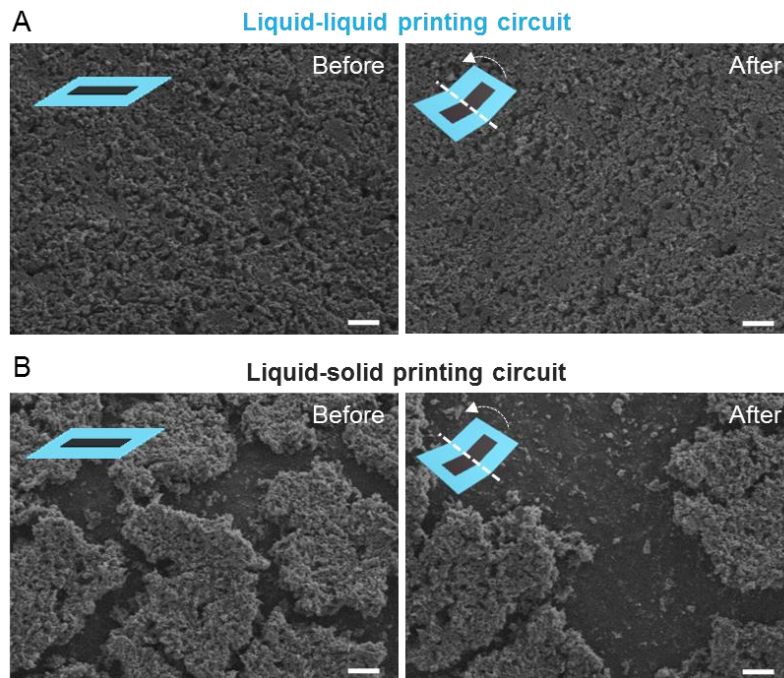


Figure S10. SEM images of liquid-liquid printing circuits (A) and liquid-solid printing circuits (B) before and after bending to 120° . Scale bar: $50\ \mu\text{m}$. Related to Figure 4.

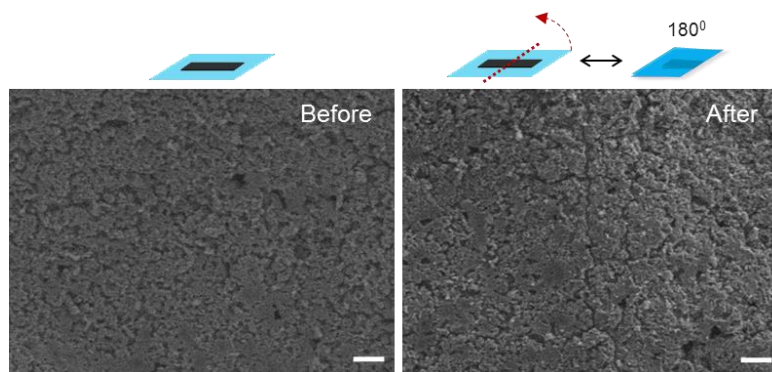


Figure S11. SEM images of liquid-liquid printing circuits before and after 1000 cycles bending to 180° . Scale bar: $50\ \mu\text{m}$. Related to Figure 4.

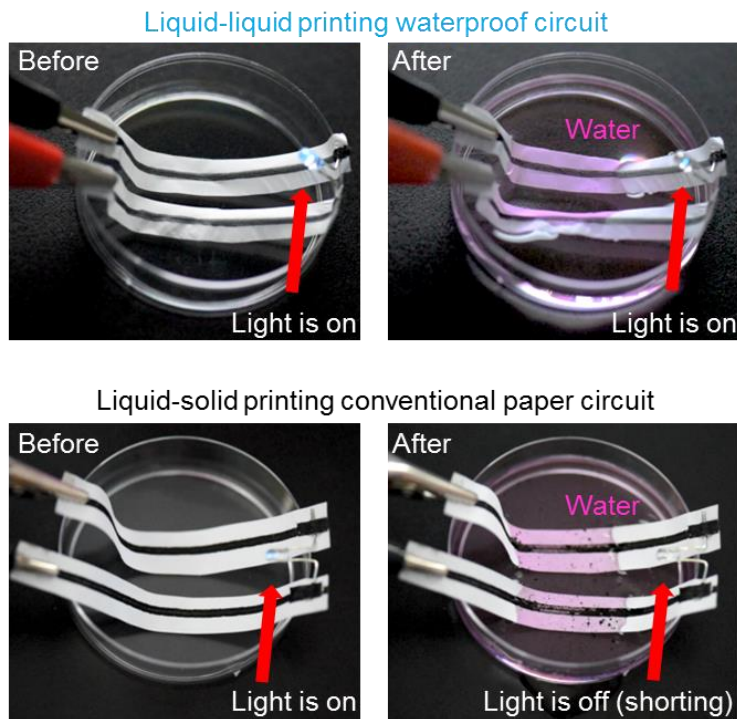


Figure S12. Waterproof of circuits based on the liquid-liquid printing technique *vs.* the conventional paper circuit. The water is the electrically conductive tap water. Comparing with the conventional paper circuit, waterproof circuit based on the liquid-liquid printing technique is much more stable. Related to Figure 4.

Table S1. Common properties of the donor liquids. Related to Figure 1.

No.	Donor liquids	Source	Density (g/mL)	Viscosity (mPa s)	CA ($^{\circ}$)	γ (mN/m)
1	Aqueous Rhodamine B	Lab-made	1.00	1.6	84.3	63.2
2	Neutral pen ink	Commercial	1.06	13.9	64.6	35.0
3	Aqueous fluorescent ink	Commercial	1.09	26.7	75.8	37.3
4	Aqueous ferrofluid	Commercial	1.39	94.1	91.2	58.3
5	Conductive donor	Lab-made	0.97	163.0	58.7	33.9

CA, contact angle. γ , surface tension, 25 $^{\circ}$ C.

Table S2. Liquid properties in Figure 2. Related to Figure 2.

Liquids	Solvents	Solutes	Density (g/mL)	Volatilization rate (mg/min)	γ (mN/m)
RB (Water)	Water	Rhodamine B	1.00	0.84	60.98
SY (Water)	Water	Sunset yellow	1.01	0.86	71.33
CM (Water)	Water	Carmine	1.01	0.77	70.41
RB (FA)	Formic acid	Rhodamine B	1.22	1.40	38.71
SY (FA)	Formic acid	Sunset yellow	1.21	0.85	38.75
RB (DMAC)	Dimethylacetamide	Rhodamine B	0.95	0.33	34.77
SY (DMAC)	Dimethylacetamide	Sunset yellow	0.95	0.26	34.34
SD (DMAC)	Dimethylacetamide	Sudan red II	0.95	0.20	34.81
SD (DMF)	Dimethylformamide	Sudan red II	0.99	0.54	36.71
RB (GLY)	Glycerin	Rhodamine B	1.27	0.00	62.31
SY (GLY)	Glycerin	Sunset yellow	1.28	0.00	63.57
SD (SO)	Shell oil	Sudan red II	0.81	0.00	28.16
PVP (FA)	Formic acid	Polyvinylpyrrolidone	1.24	1.03	38.73
PVB (Ethanol)	Ethanol	Polyvinyl butyral	0.83	1.19	22.83
PLA (DCM)	Dichloromethane	Polylactic acid	1.52	4.47	36.13
PS (THF-DMF)	Tetrahydrofuran, dimethylformamide	Polystyrene	1.03	0.25	36.26
PVDF (Acetone-DMAC)	Acetone, Dimethylacetamide	Polyvinylidene fluoride	0.92	0.21	29.22

RB: Rhodamine B; SY: sunset yellow; CM: carmine; SD: Sudan red; GLY: glycerin; SO: shell oil. DMAC: dimethylacetamide; THF: tetrahydrofuran; DMF: dimethylformamide; DCM: dichloromethane; FA: formic acid; PVDF: polyvinylidene fluoride; PS: polystyrene; PLA: polylactic acid; PVB: polyvinyl butyral; PVP: polyvinylpyrrolidone. γ , surface tension, 25 °C.

Table S3. Soluble levels of the donor solutes. Related to Figure 2.

	RB	SY	CM	SD
FA	5	5	5	5
Ethanol	5	2	2	4
DCM	5	1	1	5
THF-DMF	5	5	2	5
Acetone-DMAC	5	5	4	5

“1” denotes insoluble, “2” poor solubility, “4” unstable dissolution, and “5” dissolving completely. RB: Rhodamine B; SY: sunset yellow; CM: carmine; SD: Sudan red; FA: formic acid; DCM: dichloromethane; THF: tetrahydrofuran; DMF: dimethylformamide; DMAC: dimethylacetamide.

Table S4. The receding angle (°) of the donor liquids. Related to Figure 2.

	PVDF (Acetone-DMAC)	PS (THF-DMF)	PLA (DCM)	PVB (Ethanol)	PVP (FA)
RB (Water)	57.6	0	61.2	46.8	0
SY (Water)	48.6	0	36	37.8	0
CM (Water)	64.8	12.6	34.2	0	0
RB (FA)	32.4	0	0	0	0
SY (FA)	0	0	0	0	0
RB (DMAC)	0	0	0	0	0
SY (DMAC)	0	0	0	0	0
SD (DMAC)	0	0	0	0	0
SD (DMF)	0	0	0	0	0
RB (GLY)	0	0	97.2	0	0
SY (GLY)	0	0	55.8	0	0
SD (SO)	0	0	39.6	0	0
Water (RB)	57.6	0	61.2	46.8	0

PVDF: polyvinylidene fluoride; PS: polystyrene; PLA: polylactic acid; PVB: polyvinyl butyral; PVP: polyvinylpyrrolidone; DMAC: dimethylacetamide; THF: tetrahydrofuran; DMF: dimethylformamide; DCM: dichloromethane; FA: formic acid; RB: Rhodamine B; SY: sunset yellow; CM: carmine; SD: Sudan red; GLY: glycerin; SO: shell oil.

Table S5. Values of parameters used in the simulations in Figure 3. Related to Figure 3.

	Value	Unit	Description
c_0	0.83	Dimensionless	Mass ratio of L_{RS} to L_R in L_R flow
τ	0.00294	g/s	Mass evaporation rate of L_{RS}
k	0.001195	g/s	Mass flow rate of L_R
D_{1solv}	1×10^{-9}	m^2/s	Diffusion coefficient of the pure L_{DS} in the L_{RS}
D_{1poly}	1×10^{-12}	m^2/s	Diffusion coefficient of the pure L_{DS} in the L_{RP}
$D_0(c)$	0	m^2/s	Diffusion coefficient of ink solute in L_R
r	0.4	Dimensionless	Ratio of diffusion coefficient of ink solute and L_{DS}
Z_0	5	Dimensionless	Lower critical value in ink diffusion function
Z_1	15	Dimensionless	Upper critical value in ink diffusion function
c_{cri}	0.11	Dimensionless	Critical mass ratio of L_{RS} to L_R

L_R , the receiver liquid, was prepared by dissolving PVDF (L_{RP}) in acetone/DMAC (L_{RS}).

Table S6. Mass ratio of the receiver solvent to the overall receiver during electrospray.

Related to Figure 3.

Injection rate (mL h ⁻¹)	T (min)	Solvent (g)	Polymer (g)	<i>c</i>
3.0	6.0	0.0016	0.024	0.0625
	10.0	0.0050	0.043	0.1042
	20.0	0.0087	0.085	0.0928
	40.0	0.0234	0.183	0.1134
	50.0	0.0293	0.222	0.1166
5.1	6.0	0.0209	0.048	0.3033
	10.0	0.0497	0.078	0.3892
	20.0	0.0778	0.142	0.3540
	40.0	0.2322	0.325	0.4167
	50.0	0.1874	0.374	0.3338

c is the mass ratio of the receiver solvent (acetone/dimethylacetamide 1:1) to the overall receiver (polyvinylidene fluoride).

Transparent Methods

Materials

The materials including polyvinylidene fluoride (PVDF, M.W. 500,000, Solvay), polyvinylpyrrolidone (PVP, M.W. 130,000, Aladdin), polystyrene (PS, M.W. 100,000, Xiya), polyvinyl butyral (PVB, M.W. 9,000-120,000, Aladdin), polylactic acid (PLA, M.W. 60,000, Aldrich), polyacrylonitrile (PAN, M.W. 150,000, Sigma), graphite nanoplatelet aqueous (Aladdin), and graphene (Aladdin). N,N-Dimethylacetamide (DMAC), acetone, ethanol, tetrahydrofuran (THF), dimethylformamide (DMF), dichloromethane (DCM), and formic acid (FA) of analytical grade were obtained from Sinopharm Chemical Reagent Co., Ltd. All solutions were prepared with Milli-Q water (18.2 M Ω cm).

Donor preparation

The donor liquids include two types: one is lab-made simple, for example, an aqueous Rhodamine B (RB) donor liquid in Figure S1; the others are complex fluids, including inks in commercial pen refills (Figure S4B), lab-made composite solutions, and lab-made suspensions (Figure S9A). RB aqueous solution used in Figure S1 was prepared by dissolving RB powders in water with a final concentration of 0.1 mg mL⁻¹. For a conductive donor preparation, the graphene powders were dispersed in graphite nanoplatelet aqueous with a concentration of 10 mg mL⁻¹. The PVP was dispersed in ethanol with a concentration of 8% (wt/v). The two above mentioned solutions were mixed thoroughly under ultrasound to obtain the conductive donor (Figure S9A, Movie S2). Common properties of the donor liquids are listed in table S1.

Donor patterns preparation

The donor pattern was drawn onto the surface of a substrate by using a lettering robot

manipulator (Steamduino, China) with multiple donor liquids. A neutral pen (MG-2180, M&G Chenguang, China) was used in the experiments in Figure 3 and the black outlines of the colorful printing in Figure 4C and Figure S7B. The density and viscosity of the donor liquid are 1.06 g mL^{-1} and 13.9 mPa s at 0.1 s^{-1} shear rate, respectively (see Figure S4B). A neutral red pen (Deli 34567#, DeLi Group Co., Ltd., China) is used in Figure 1B. And the density of the ink is 1.05 g mL^{-1} . Aqueous fluorescent pens (Uni, PUS-102T, Japan) are used in Figure 4A and 4B, Figure S5, and Movie S1. Watercolor pens (ZCP24308, M&G Chenguang, China) with water-based color dyes are used for the colorful areas in Figure 4C and Figure S7B.

For the preparation of the flexible circuits, a conductive donor was contained in a syringe (2.5 mL) attached to a micro nozzle (23G). A Harvard Apparatus PHD ULTRATM Syringe Pump was used to extrude the conductive donor liquid onto the surface of an aluminum foil (surface energy 38.9 mN/m), solid PVDF (surface energy 32.6 mN/m) or A4 paper (for preparing conventional paper circuit in Figure S12) with a flow rate of $100 \text{ }\mu\text{L min}^{-1}$.

Receiver liquids preparation

PVDF (acetone-DMAC) was chosen for a typical receiver liquid, because of its high compatibility with various types of liquid donors (see Figure 2A). The PVDF (acetone-DMAC) solution (8% wt/v, density 0.89 g mL^{-1} , viscosity 194.0 mPa s at 0.1 s^{-1} shear rate, Figure S4A) was prepared by dissolving PVDF in acetone/DMAC (1:1). The fabricating process was performed with an ET-2535H electrospray machine (ET-2535H, Ucalery, China). The solution was injected through a 20G needle (injection rate $0.085 \sim 12.0 \text{ mL h}^{-1}$, applied voltage $8 \sim 13 \text{ kV}$, the distance between the tip of the needle and the

target 13 cm). PVDF solidifies during the volatilization of the receiver solvents. The whole process was conducted at 25 °C ~ 30 °C and 30% ~ 41% relative humidity for 0.1 ~ 2 h except otherwise specified. After the receiver solvent is completely volatilized, the solidification is completed. For Figure 1 B, after electro spray, both partially solidified and full solidified PVDF with transfer printed donor pattern could be easily detached from the substrate. A scanning electron microscope (SEM) image of the solid state of PVDF is shown in Figure S3D. Other receivers (Table S2) include 20% (wt/v) polystyrene with THF/DMF 1:1, 12% (wt/v) PLA with DCM, 6% (wt/v) PVB with ethanol, 10% (wt/v) PVP with FA.

In Figure 3B, we set a series of injection flow rates from 0.7 mL h⁻¹ to 12.0 mL h⁻¹ and the total injection volumes remain at 0.857 mL. Optical photos were taken to record the line width before and after the electro spray. In Figure 3C, the injection flow rate was set to 5.1 mL h⁻¹. Optical photos were taken to record the line width in real time (from 0 min to 51.5 min). For Figure S1, PVDF (acetone-DMAC) was first prepared according to the typical electro spray process described above. After the contact of RB liquid donor and the PVDF (acetone-DMAC) receiver, absorbent papers were used to absorb the excess RB liquid above. The printing process was operated in air with continuous volatilization of the receiver solvents. The PVDF was solidified along with the volatilization of the receiver solvents. The PVDF is full solidified when the solvent is completely volatilized. Then the printed materials were rinsed with DI water for three times and were dried in air.

Flexible circuits preparation

For liquid-liquid printing (LLP) circuit materials, the solutions were 8% ~ 12% (wt/v)

PVDF with the injection rate 10 mL h^{-1} for 10 ~15 min following by 3.5 mL h^{-1} for 40 min. For waterproof circuits' preparation, after the LLP circuit was peeled off from the aluminum foil, we turned them over for another electrospray process (injection rate 3.5 mL h^{-1} for 40 min). The obtained waterproof circuit (thickness $\sim 85 \text{ }\mu\text{m}$) was encapsulated between two layers of PVDF. For liquid-solid printing circuits, the conductive donor was directly written on the surface of PVDF (Movie S2).

Characterizations

The viscosity of the liquids was measured at $25 \text{ }^\circ\text{C}$ using Rheo-Microscope MCR302 (Anton Paar Co., Austria). Viscosities as well as other common properties of our donor liquids were summarized at Table S1. Liquids volatilization rate tests were measured with $\sim 10 \text{ }\mu\text{L}$ liquid vaporizing in air to demo the electrospray process, at 25°C and $38\% \pm 3\%$ relative humidity. The liquids were dropped onto aluminum foils with an area of $3 \text{ cm} \times 3 \text{ cm}$. The volatilization time was recorded until the liquids totally drying. The volatilization rate is the loss of weight of the liquids per minutes. The special affinity is denoted for the receding angle (Wang et al., 2015) divided by the solubility level of the donor solute in the receiver liquid (Table S3). For the tests of the soluble levels of the donor solutes in the receiver solvents, 2.0 mg donor solutes were added into 5.0 mL solvent following whirlpool concussion to full dissolution ($22 \text{ }^\circ\text{C}$).

The relative conductance of the printing circuits was obtained by using a source meter (2400, Keithley, USA). A voltage of 10 V was applied to the graphene line with the length of 3.5 cm and the width of 2 mm , and the current value was recorded. Fluorescent images were obtained by a TCS SP5 beam scanning confocal microscope (Leica Microsystems CMS GmbH, Germany). Zoomed-in view of the surface

morphology of the LLP and LSP circuits (Figure 4G right) was performed by a laser microscopic system (Keyence, VK-X250K). The SEM images were obtained by a field-emission scanning electron microscope Hitachi s-4800 (Hitachi, Japan). The contact angle and the receding angle measurements were performed by a contact angle measurement system OCA100 (Dataphysics, Germany) at room temperature (*i.e.*, 20 °C ~ 25 °C) with ~ 22% relative humidity (Sheng et al., 2018). During the measurements, small droplets of water (5 µL) were placed on multiple areas on the surface of the samples. Surface tension and surface energy were measured by the pendant drop method and the Owens, Wendt, Rabel and Kaelble (OWRK) method (Owens and Wendt, 1969), respectively. For the receding angle measurements (Wang et al., 2015), the receiver liquids were first placed on the aluminum foil following by contact with the donor liquids. The value of the contact angle, the receding angle and the surface tension was an average of at least three independent measurements.

Stability tests

The liquid-liquid printed materials were immersed into 1M HCl, 1M NaOH, boiling water or 95% alcohol for 10 min. The immersion time for 36.5% NaCl was two days. After the treatment, the printed materials were drawn from the solutions and rinsed with DI water for 5 min.

Theoretical modeling

We define c_0 as the mass ratio of the L_{RS} in the sprayed L_R flow. When L_R is sprayed with the mass flow rate k , the solvent (L_{RS}) in L_R partly evaporates while all polymers (L_{RP}) stay on the surface of the substrate. Here, the mass evaporation rate of L_{RS} is assumed to be a constant during the process, which is denoted as τ . The mass ratio of L_{RP}

c is different from the sprayed L_R c_0 . Here, we assume the sprayed L_R mixes uniformly with the existing solution in the substrate. From the mass conservation of L_R and L_{RS} ,

$$h(t) + kdt - \tau c(t)dt = h + dh \quad (1)$$

$$c(t)h(t) + kc_0dt - \tau c(t)dt = (c + dc)(h + dh) \quad (2)$$

where h is the mass of L_R membrane. The corresponding differential equations can be easily derived,

$$\frac{dh}{dt} = k - \tau c \quad (3)$$

$$\frac{dc}{dt} = \frac{1}{h}(kc_0 - kc - \tau c + \tau c^2) \quad (4)$$

From Fick's second law of diffusion, the governing equations for g and f are

$$\frac{\partial g}{\partial t} = \nabla(a(c)\nabla g) \quad (5)$$

$$\frac{\partial f}{\partial t} = \nabla(Z(g/f, c)\nabla f) \quad (6)$$

where g and f are the density of the donor solvent and the density of the donor ink solute, respectively, a and Z are the diffusion coefficients of donor solvent and donor ink solutes in the overall receiver. The numerical simulation is computed in COMSOL Multiphysics 5.3 with the parameters listed in Table S5 and S6. The diffusion coefficients values are the typical values of the diffusivity of the liquid in liquid and liquid in solid for the contents used in the experiments.

It needs to be mentioned that the k value in the Table S5 is proportional to the flow rate. The value of 5.1 mL h^{-1} listed in the Table S6 is used to plot Figure 3C.

Supplemental references

Owens, D.K., and Wendt, R.C. (1969). Estimation of the surface free energy of polymers. *J. Appl. Polym. Sci.* *13*, 1741-1747.

Sheng, Z., Wang, H., Tang, Y., Wang, M., Huang, L., Min, L., Meng, H., Chen, S., Jiang, L., and Hou, X. (2018). Liquid gating elastomeric porous system with dynamically controllable gas/liquid transport. *Sci. Adv.* *4*, eaao6724.

Wang, L., Li, F., Kuang, M., Gao, M., Wang, J., Huang, Y., Jiang, L., and Song, Y. (2015). Interface Manipulation for Printing Three-Dimensional Microstructures Under Magnetic Guiding. *Small* *11*, 1900-1904.